Master-Slave Second Order Sliding Mode Control for Microgrids

Michele Cucuzzella, Gian Paolo Incremona and Antonella Ferrara

***Abstract*— This paper deals with the design of advanced control strategies of sliding mode type for microgrids. Each distributed generation unit (DGu), constituting the considered microgrid, can work in both grid-connected and islanded operation mode. The DGu is affected by load variations, nonlinearities and unavoidable modelling uncertainties, because of the presence of a voltage-sourced-converter (VSC) as interface with the main grid. This kind of uncertainty terms makes the sliding mode controller perfectly fitting the control problem to solve. In particular, a second order sliding mode (SOSM) control scheme, belonging to the class of Suboptimal SOSM control, is proposed. Moreover, in order to face some undesired overshoot on the currents fed into the load, due to the reconnection to the main grid, as well as to step variations of current references, a constrained SOSM control is designed. Simulation results confirm that the proposed robust controllers provide closed-loop performance complying with the IEEE recommendations for power systems.**

I. Introduction

Recently, the increasing of energy sources of renewable type has given rise to a new paradigm in the power generation and in the realization of plants. Particularly, much smaller and geographically distributed generation units (DGus) are realized [1]. Moreover, this new technological alternative allows one to achieve technical, economical and environmental benefits, in terms of energy efficiency and reduced carbon emissions [2]. DGus also improve the service quality and continuity [3], by supplying at least a portion of the load, even after being disconnected from the main grid [4].

In the literature, a set of multiple mutual connected DGus, which are usually strictly close to the energy consumers, is identified as a "microgrid" [5]–[7] . The latter, characterized by some intelligent computation and metering capability, can be considered as the basic unit of the so-called "smart grid" [8]. Because of the intermittence, randomness and the uncertainty caused by meteorological factors, it is difficult to integrate renewable energy sources directly into the main grid. This is the reason why voltage control, fault detection, reliability, and power losses are among the issues to solve in order to integrate DGus into the distribution network [9].

In [10], a structurally simple controller is proposed to stabilize a DGu in spite of the presence of some uncertainties. Moreover, an integral oscillator to control the frequency and a voltage closed-loop control in islanded mode are used. A master-slave configuration of two degree-of-freedoms with optimal control is considered in [11], while recently, new decentralized control schemes for islanded configurations are proposed in [12]. In particular, a Plug-and-Play (PnP) algorithm is introduced, but traditional not robust local controllers are used.

This is the final version of the accepted paper submitted for inclusion in the Proceedings of the American Control Conference, Jul., 2015.

In this paper, a master-slave scheme with advanced control strategies, which belong to the class of the so-called Suboptimal Second Order Sliding Mode (SOSM) algorithms, is proposed [13]–[16]. The SOSM algorithm has good properties in terms of chattering alleviation and stability performance. The sliding mode is enforced on a suitable designed sliding manifold from a reaching time after which the robustness of the controlled system is proved. In order to alleviate some overshoot of the currents fed into the load, also a constrained version of Suboptimal SOSM control for microgrids is designed in analogy with [17]. The effectiveness of the proposed approaches has been assessed in simulation, relying on a model of a microgrid with three DGus.

The present paper is organized as follows. In Section II the considered DGu architecture is described, while in Section III the control problem is formulated. The proposed master-slave Suboptimal SOSM control strategies are presented in Section IV. The stability analysis is discussed in Section V, while simulation results are presented in Section VI. Some conclusions (Section VII) end the paper.

II. Preliminary Issues

For the readers' convenience, a brief description of the so-called DGu is hereafter reported.

A. The Distributed Generation Unit (DGu)

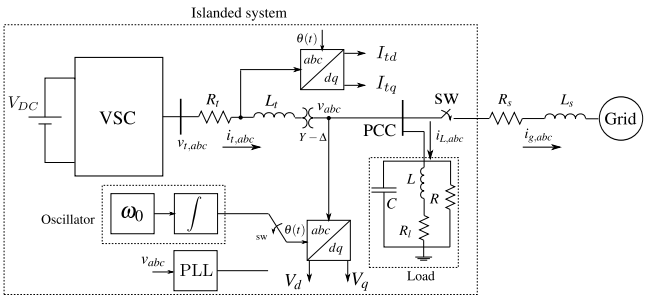

Fig. 1. Simplified schematic single-line diagram of a DGu.

Consider the schematic representation of a typical DGu in Fig. 1. The first element (V_{DC}) is typically an energy source of renewable type, which can be represented by a direct current (DC) voltage source. The latter is connected to the so-called voltage-sourced-converter (VSC). In our case this is a pulse width modulation (PWM) inverter. The VSC and a resistive-inductive (R_tL_t) filter, able to extract the fundamental frequency of the converter output voltage, are the interface

TABLE I
ELECTRICAL PARAMETERS OF THE DGU IN FIG. 1

Quantity	Value	Description
V_{DC}	1000 V	DC voltage source
f_c	10 kHz	PWM carrier frequency
R_t	40 mΩ	VSC filter resistance
L_t	10 mH	VSC filter inductance
R	4.33 Ω	Load resistance
L	100 mH	Load inductance
C	1 pF	Load capacity
R_s	0.1 Ω	Grid resistance
f_0	60 Hz	Nominal grid frequency
V_n	120 V	Nominal grid phase-voltage (RMS)

medium with the main grid. The electrical connection point of the DGu to the main grid is the point of common coupling (PCC) where a local three-phase parallel resistive-inductive-capacitive (RLC) load is connected. The main grid is represented by a resistive-inductive (R_sL_s) impedance and by an alternate current (AC) voltage source. The parameters of the system considered in this paper (see Fig. 1) are reported in Table I. The latter have been selected in analogy with a realistic case (see for instance [19]).

B. Grid-Connected Operation Mode (GCOM)

In this operation mode, the PCC voltage magnitude and frequency are dictated by the main grid. Thus, the system operates in stiff synchronization with the grid by using the so-called phase-locked-loop (PLL), which provides the reference angle θ for the Park's transformation [18]. In order to operate the lock with the main grid, a proportion-integral (PI) controller steers to zero the quadrature voltage component V_q. In such a case, the active and reactive power are equal to $P = 3/2 V_d I_{td}$ and $Q = -3/2 V_d I_{tq}$ respectively, with V_d being the direct component of load voltage v_{abc}, I_{td} and I_{tq} being the direct and quadrature components of the current $i_{t,abc}$. Hence, the DGu works in current control mode in order to supply P_{ref} and Q_{ref}, which are the corresponding active and reactive power references, depending only on the direct and quadrature current component, respectively.

According to the Park's transformation, the AC currents generated by the VSC are referred to a synchronous rotating dq-frame and regulated like DC signals. The direct and quadrature components are compared with the corresponding references to compute the errors, which are sent to the current controller in order to generate the voltage references. The latter are transformed back into the stationary abc-frame according to the inverse Park's transformation, and used by the VSC.

C. Islanded Operation Mode (IOM)

In this case, the circuit breaker (named SW in Fig. 1) is open. Because of the power mismatch between the DGu and the load, the PCC voltage and frequency could deviate from the rated values. Therefore, in IOM the DGu must switch to the voltage control mode and provide a constant voltage to the local load. The control scheme employs an internal oscillator with a constant angular frequency equal to the nominal one, namely $\omega_0 = 2\pi f_0$, to generate the modulating signals. The VSC is controlled by the voltage controller, according to the synchronous reference dq-frame. The voltage control signals are transformed back into the stationary abc-frame according to the inverse Park's transformation, and used by the VSC.

The transition from the GCOM to the IOM has to be smoothly performed to avoid system performance degradation. Thus, when the voltage control is activated, the instantaneous phase angle, provided by the PLL, in the current control mode, must be used as the initial condition for the internal oscillator. To avoid hard transients, also before the reconnection to the main grid, the PCC voltage must be resynchronized with the grid voltage, for instance as proposed in [19].

III. PROBLEM FORMULATION

Consider the scheme of the DGu in Fig. 1 and assume the system symmetric and balanced. Moreover, consider the DGu in IOM, such that, according to the abc-frame, the model is

$$\begin{cases} i_{t,abc} = \frac{1}{R} v_{abc} + i_{L,abc} + C \frac{dv_{abc}}{dt} \\ v_{t,abc} = L_t \frac{di_{t,abc}}{dt} + R_t i_{t,abc} + v_{abc} \\ v_{abc} = L \frac{di_{L,abc}}{dt} + R_l i_{L,abc} \end{cases} \tag{1}$$

where $i_{L,abc}$ is the current flowing on the load inductance, while $v_{t,abc}$ is the VSC output voltage. System (1) can be referred to the synchronous rotating dq-frame by applying the Clarke's and Park's transformations. Then, the state-space representation of (1) results in being

$$\begin{cases} \dot{x}_1(t) = -\frac{1}{RC}\ x_1(t) + \omega_0\ x_2(t) + \frac{1}{C}\ x_3(t) - \frac{1}{C}\ x_5(t) \\ \dot{x}_2(t) = -\omega_0\ x_1(t) - \frac{1}{RC}\ x_2(t) + \frac{1}{C}\ x_4(t) - \frac{1}{C}\ x_6(t) \\ \dot{x}_3(t) = -\frac{1}{L_t}\ x_1(t) - \frac{R_t}{L_t}\ x_3(t) + \omega_0\ x_4(t) + \frac{1}{L_t}\ u_1(t) \\ \dot{x}_4(t) = -\frac{1}{L_t}\ x_2(t) - \omega_0\ x_3(t) - \frac{R_t}{L_t}\ x_4(t) + \frac{1}{L_t}\ u_2(t) \\ \dot{x}_5(t) = \frac{1}{L}\ x_1(t) - \frac{R_l}{L}\ x_5(t) + \omega_0\ x_6(t) \\ \dot{x}_6(t) = \frac{1}{L}\ x_2(t) - \omega_0\ x_5(t) - \frac{R_l}{L}\ x_6(t) \\ y_1(t) = x_1(t) \\ y_2(t) = x_2(t) \end{cases} \tag{2}$$

where $x = [V_d\ V_q\ I_{td}\ I_{tq}\ I_{Ld}\ I_{Lq}]^T \in \mathcal{X} \subset \mathbb{R}^6$ is the state variables vector, $u = [V_{td}\ V_{tq}]^T \in \mathcal{U} \subset \mathbb{R}^2$ is the input vector and $y_{IOM} = [V_d\ V_q]^T \in \mathbb{R}^2$ is the output vector. Likewise, it can be found the state space model for the system in GCOM, the output vector of which is $y_{GCOM} = [I_{td}\ I_{tq}]^T \in \mathbb{R}^2$.

The control objective consists in designing a robust control strategy, so as to guarantee that the controlled electrical signals follow their references, while ensuring satisfactory closed-loop performance even in presence of uncertainties.

IV. THE PROPOSED SOSM CONTROL STRATEGY

The adopted methodology to solve the aforementioned control problem is SOSM control [20]. In particular, a strategy of suboptimal type is designed.

In Fig. 2, the proposed control scheme with two DGus is illustrated. It has a master-slave structure. Indeed, the DGu with the most energy capacity acts as a Master (DGu_M), while the other as a Slave (DGu_S). In GCOM, all DGus regulate their own active and reactive power with the conventional dq current control. When an islanding event occurs, only the

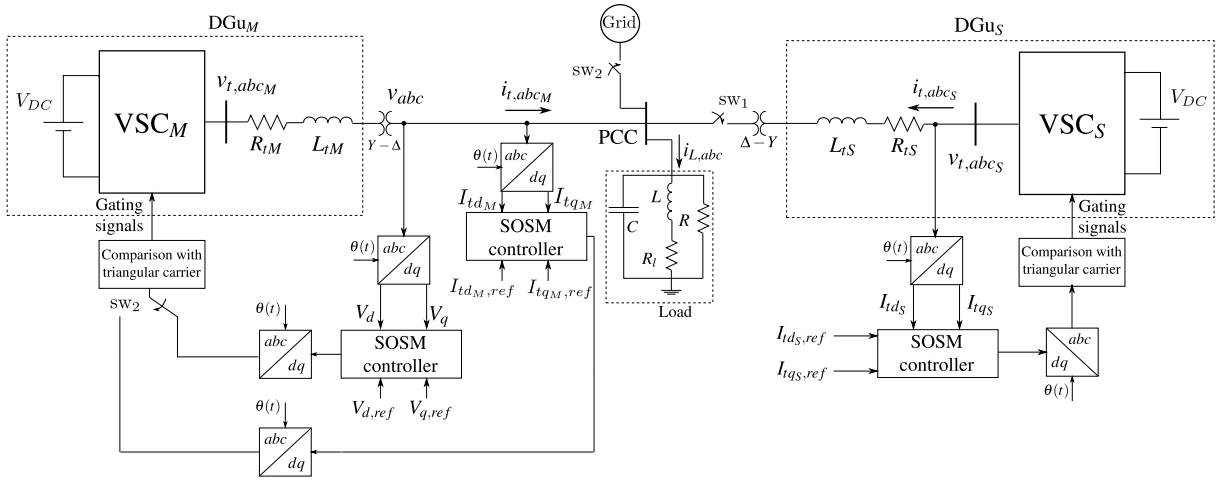

Fig. 2. Representation of the master-slave system with SOSM controllers.

DGu$_M$ switches to the voltage control mode and becomes responsible to keep the microgrid voltage constant with respect to its reference value. Note that, this architecture can be extended to the case with several DGus, each of which is independently controlled in a decentralized manner [21].

Consider the IOM state-space model (2) and assume that the so-called "sliding variables" are equal to $\sigma_{1_{IOM}}(t) = y_{1_{IOM},ref} - y_{1_{IOM}}(t)$ and $\sigma_{2_{IOM}}(t) = y_{2_{IOM},ref} - y_{2_{IOM}}(t)$. Since the relative degree r of the system is equal to 2, a SOSM control naturally applies [13], [14]. According to SOSM control theory, we need to define the so-called auxiliary variables $\xi_{1,1_{IOM}}(t) = \sigma_{1_{IOM}}(t)$ and $\xi_{2,1_{IOM}}(t) = \sigma_{2_{IOM}}(t)$ such that the corresponding auxiliary systems can be expressed as

$$\begin{cases} \dot{\xi}_{i,1_{IOM}}(t) = \xi_{i,2_{IOM}}(t) \\ \dot{\xi}_{i,2_{IOM}}(t) = f_{i_{IOM}}(x(t)) + g_{i_{IOM}} u_{i_{IOM}}(t) \end{cases} \quad i = 1,2 \quad (3)$$

where $\xi_{i,2_{IOM}}(t), i = 1,2$, are assumed unmeasurable, and

$$\begin{aligned} f_{1_{IOM}}(x(t)) &= (\omega_0^2 - \tfrac{1}{(RC)^2} + \tfrac{1}{L_tC} + \tfrac{1}{LC})x_1(t) + \tfrac{2\omega_0}{RC}x_2(t) \\ &\quad + (\tfrac{1}{RC^2} + \tfrac{R_t}{L_tC})x_3(t) - \tfrac{2\omega_0}{C}x_4(t) \\ &\quad - (\tfrac{1}{RC^2} + \tfrac{R_l}{LC})x_5(t) + \tfrac{2\omega_0}{C}x_6(t) \\ f_{2_{IOM}}(x(t)) &= -\tfrac{2\omega_0}{RC}x_1(t) + (\omega_0^2 - \tfrac{1}{(RC)^2} + \tfrac{1}{L_tC} + \tfrac{1}{LC})x_2(t) \\ &\quad + \tfrac{2\omega_0}{C}x_3(t) + (\tfrac{1}{RC^2} + \tfrac{R_t}{L_tC})x_4(t) \\ &\quad - \tfrac{2\omega_0}{C}x_5(t) - (\tfrac{1}{RC^2} + \tfrac{R_l}{LC})x_6(t) \\ g_{i_{IOM}} &= \tfrac{1}{L_tC}\ , \quad i = 1,2 \end{aligned} \quad (4)$$

are allowed to be uncertain with bounds $|f_{i_{IOM}}(\cdot)| \leq F_{i_{IOM}}$ and $G_{i,m_{IOM}} \leq |g_{i_{IOM}}| \leq G_{i,M_{IOM}}$, $F_{i_{IOM}}$, $G_{i,m_{IOM}}$ and $G_{i,M_{IOM}}$ being positive constants.

Analogously, in GCOM, the sliding variables are chosen by considering the error of I_{td} and I_{tq}. In this case, the natural relative degree of the system is equal to 1. So, a first order sliding mode controller would be adequate. Yet, in order to alleviate the chattering phenomenon [22]–[26], i.e. high frequency oscillations of the controlled variable, which can be dangerous in terms of harmonics affecting the electrical signals, the SOSM control is used also in this case, by artificially increasing the relative degree of the system. Specifically, by defining the sliding variables as $\sigma_{1_{GCOM}}(t) = y_{1_{GCOM},ref} - y_{1_{GCOM}}(t)$, $\sigma_{2_{GCOM}}(t) = y_{2_{GCOM},ref} - y_{2_{GCOM}}(t)$ and the auxiliary variables as $\xi_{1,1_{GCOM}}(t) = \sigma_{1_{GCOM}}(t)$, $\xi_{2,1_{GCOM}}(t) = \sigma_{2_{GCOM}}(t)$, one has

$$\begin{cases} \dot{\xi}_{i,1_{GCOM}}(t) = \xi_{i,2_{GCOM}}(t) \\ \dot{\xi}_{i,2_{GCOM}}(t) = f_{i_{GCOM}}(x(t),u(t)) + g_{i_{GCOM}} w_{i_{GCOM}}(t) \\ \dot{u}_{i_{GCOM}}(t) = w_{i_{GCOM}}(t) \end{cases} \quad i = 1,2 \quad (5)$$

where $\xi_{i,2_{GCOM}}(t), i = 1,2$, are assumed unmeasurable, and

$$\begin{aligned} f_{1_{GCOM}}(x(t),u(t)) &= -(\tfrac{1}{RL_tC} + \tfrac{R_t}{L_t^2})x_1(t) + \tfrac{2\omega}{L_t}x_2(t) \\ &\quad + (\omega^2 + \tfrac{1}{L_tC} - \tfrac{R_t^2}{L_t^2})x_3(t) + \tfrac{2\omega R_t}{L_t}x_4(t) \\ &\quad - \tfrac{1}{L_tC}x_5(t) - \tfrac{1}{L_tC}x_7(t) + \tfrac{R_t}{L_t^2}u_1(t) - \tfrac{\omega}{L_t}u_2(t) \\ f_{2_{GCOM}}(x(t),u(t)) &= -\tfrac{2\omega}{L_t}x_1(t) - (\tfrac{1}{RL_tC} + \tfrac{R_t}{L_t^2})x_2(t) \\ &\quad - \tfrac{2\omega R_t}{L_t}x_3(t) + (\omega^2 + \tfrac{1}{L_tC} - \tfrac{R_t^2}{L_t^2})x_4(t) \\ &\quad - \tfrac{1}{L_tC}x_6(t) - \tfrac{1}{L_tC}x_8(t) + \tfrac{\omega}{L_t}u_1(t) + \tfrac{R_t}{L_t^2}u_2(t) \\ g_{i_{GCOM}} &= \tfrac{1}{L_t}\ , \quad i = 1,2 \end{aligned} \quad (6)$$

are allowed to be uncertain with bounds $|f_{i_{GCOM}}(\cdot)| \leq F_{i_{GCOM}}$ and $G_{i,m_{GCOM}} \leq |g_{i_{GCOM}}| \leq G_{i,M_{GCOM}}$, $F_{i_{GCOM}}$, $G_{i,m_{GCOM}}$ and $G_{i,M_{GCOM}}$ being positive constants. Note that, the existence of these bounds is true in practice due to the fact that $f_{i_\nu}(\cdot)$, ν being the subscript IOM or GCOM, depend on electrical signals related to the finite power of the system and g_{i_ν} are constants. The control laws proposed to steer $\xi_{i,1_\nu}(t)$ and $\xi_{i,2_\nu}(t)$ to zero in a finite time in spite of the uncertainties, in analogy with [13], can be expressed as follows

$$u_{i_{IOM}}(t) = -\alpha_{i_{IOM}} U_{i_{IOM},max}\, \mathrm{sgn}(\xi_{i,1_{IOM}}(t) - \tfrac{1}{2}\xi_{i,1_{IOM},max}) \quad (7)$$

$$w_{i_{GCOM}}(t) = -\alpha_{i_{GCOM}} U_{i_{GCOM},max}\, \mathrm{sgn}(\xi_{i,1_{GCOM}}(t) - \tfrac{1}{2}\xi_{i,1_{GCOM},max}) \quad (8)$$

with bounds

$$U_{i_{V,max}} > \max\left(\frac{F_{i_V}}{\alpha^*_{i_V} G_{i,m_V}}; \frac{4F_{i_V}}{3G_{i,m_V} - \alpha^*_{i_V} G_{i,M_V}}\right) \tag{9}$$

$$\alpha^*_{i_V} \in (0,1] \cap \left(0, \frac{3G_{i,m_V}}{G_{i,M_V}}\right) \tag{10}$$

Note that, in GCOM, the SOSM algorithm requires that the discontinous controls are $w_{i_{GCOM}}$, $i = 1,2$, which only affect $\ddot{\sigma}_{i_{GCOM}}$, but not $\dot{\sigma}_{i_{GCOM}}$, so that the chattering is alleviated, and the controls actually fed into the plant are continuous. To provide a similar chattering alleviation effect also in IOM, a first order linear filter is applied to the discontinuous control variable in practical implementation, so as to exploit the "equivalent control" concept illustrated in [27]. Furthermore, in GCOM, in order to face some undesired overshoot on the currents, due to the reconnection to the main grid, as well as step variations of current references, a constrained SOSM (SOSM$_c$) is used. According to [17], this is able to fulfill the constraints imposed on $\sigma_{i_{GCOM}}$ and $\dot{\sigma}_{i_{GCOM}}$, which physically represent the currents errors and their time derivatives.

V. Stability Analysis

With reference to the proposed SOSM control approach, the following result can be proved. For the sake of brevity the corresponding proofs are omitted.

Theorem 1: In the IOM and GCOM case, by applying the control laws (7) and (8) with bounds (9)-(10), respectively, the sliding variables $\sigma_{1_V}(t)$ and $\sigma_{2_V}(t)$, V being the subscript IOM or GCOM depending on the case, are steered to zero in a finite time.

Now, consider the IOM case. Let $e = [e_1,\ e_2,\ e_3,\ e_4,\ e_5,\ e_6]^T$ denote the state of the error system, with $e_j = x_{j,ref} - x_j,\ j = 1,\ldots,6$, x_j being the state variables of (2). With reference to the error system, the following result can be proved.

Theorem 2: Consider system (2) in IOM and variables $\sigma_{1_{IOM}}(t)$, $\sigma_{2_{IOM}}(t)$ controlled via the SOSM algorithm in (7) with bounds (9)-(10). $\forall t \geq t_r$, t_r being the time instant when $\sigma_{1_{IOM}}$, $\dot{\sigma}_{1_{IOM}}$, $\sigma_{2_{IOM}}$, $\dot{\sigma}_{2_{IOM}}$ are identically zero, $\forall x(t_r) \in \mathcal{X}$, then the origin of the error system state space is a finite time stable equilibrium point.

By virtue of the use of the SOSM control approach, the designed control system turns out to be naturally robust with respect to any uncertainty included in $f_{i_V}(\cdot)$, g_{i_V}, $i = 1,2$. It is furthermore interesting to analyze the robustness of the proposed control approach versus disturbances or uncertainties, gathered in a signal $u_{d_{VSC}}(t)$, due to the presence of the VSC in the DGu. To this end, let us consider the system in IOM and in GCOM expressed as

$$\dot{x}_V(t) = A_V x_V(t) + B_V u_V(t) + u_{d_{VSC_V}}(t) \tag{11}$$

where, we assume $u_{d_{VSC_V}}(t) = B_V h_{VSC}(t)$ and the physical bound $\|h_{VSC}(t)\| \leq h_{VSC_{max}}$ with $h_{VSC_{max}}$ being a positive constant. Note that, the associate auxiliary systems can be rewritten as in (3) and (5), replacing $f_{i_V}(\cdot)$ with $\bar{f}_{i_V}(\cdot)$, $i = 1,2$, to include the additive term $u_{d_{VSC}}(t)$, with bounds $|\bar{f}_{i_V}(\cdot)| \leq \bar{F}_{i_V}$, $\bar{F}_{i_{IOM}}$ and $\bar{F}_{i_{GCOM}}$ being positive constants. Now, the following result can be proved.

Theorem 3: System (11) in IOM and in GCOM, controlled by applying (7) and (8) with bounds (9)-(10), respectively, with $U_{i_{V,max}}$ in (9) replaced by $\bar{U}_{i_{V,max}}$, $\forall t \geq t_r$ and $x(t_r) \in \mathcal{X}$, is robust with respect to the uncertain term h_{VSC}.

VI. Simulations

In this section, the proposed control strategies are tested in simulation relying on a microgrid with three DGus, under different conditions. According to the values reported in Table I, we obtain the bounds $\bar{F}_{1_{IOM}} = 1 \times 10^{12}$, $\bar{F}_{2_{IOM}} = 4 \times 10^{10}$, $\bar{F}_{1_{GCOM}} = 4.5 \times 10^{9}$, $\bar{F}_{2_{GCOM}} = 2.5 \times 10^{7}$, $G_{i_{IOM}} = 1 \times 10^{8}$ and $G_{i_{GCOM}} = 1 \times 10^{2}$, $i = 1,2$. The SOSM parameters have been chosen equal to $U_{i,max} = 5 \times 10^{7}$, $\alpha = 1$ and $\alpha^* = 0.9$ in both IOM and GCOM, and for all the simulations the sampling time has been fixed equal to $T_s = 1 \times 10^{-6}$ s. The considered additional load absorbs an active and reactive power equal to P =25 kW and Q =1.5 kvar.

A. Transition To and From an Islanding Event

The transition time instants are imposed equal to $t_{isl} = 0.1$ s and $t_{grid} = 0.3$ s, in which the microgrid is islanded from and reconnected to the main grid, respectively. Fig. 3 illustrates the total currents injected into the main grid, both in case of SOSM and SOSM$_c$ control. Note that, the SOSM$_c$ algorithm avoids undesired overshoot on currents at $t = 0.3$ s, when the microgrid is reconnected to the main grid, and at $t = 0.35$ s, when $I_{td_M,ref}$ is stepped up from 60 A to 90 A. For this reason, the following simulations have been performed by using the SOSM$_c$ algorithm in GCOM and the SOSM one in IOM. Finally, in Table II the root mean square error of the controlled variables I_{td_M}, I_{tq_M} in GCOM, and V_d and V_q in IOM are reported, showing that the proposed SOSM$_c$ controller in GCOM and the SOSM controller in IOM are more robust and performant than the traditional PI controller. Note that the gains of PI controllers have been tuned relying

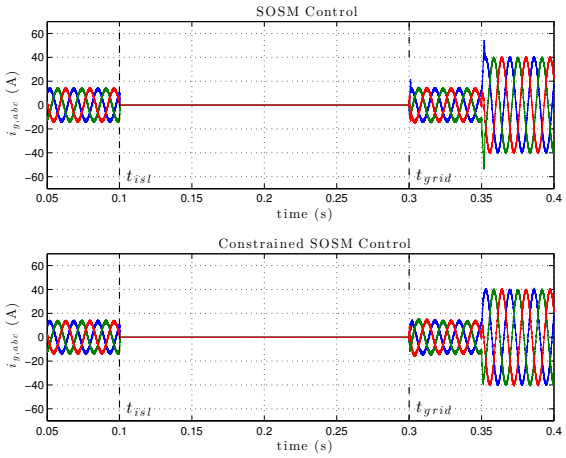

Fig. 3. Performance evaluation of SOSM and SOSM$_c$ control, comparing the instantaneous currents injected into the main grid.

TABLE II

RMS VALUES OF CURRENTS AND VOLTAGES ERROR

Configuration	PI	SOSM	SOSM$_c$
GCOM	100%	65.2%	59.5%
IOM	100%	17.5%	-

on the standard Ziegler-Nichols method to obtain a satisfactory behaviour, given the type of control, of the controlled system.

B. Robustness to Unknown Load Dynamics

Under balanced conditions in IOM, consider the addition of a purely resistive load which absorbs an active power of 3 kW. The resistive load is equally added in the three phases, such that the resulting load is still balanced. The load increase is imposed from $t = 0.15$ s to $t = 0.25$ s. Fig. 4 shows that the designed controller is robust with respect to unknown load dynamics. Indeed, the DGu$_M$ increases the delivered current to supply the added load, while keeping the load voltage constant equal to its reference value.

C. Performance under Unbalanced Load Conditions

While the system is operating in IOM under balanced load conditions, at $t = 0.15$ s resistive and inductive loads are added, such that the resulting load becomes unbalanced. The relative values of the additional loads with respect to the nominal three-phase parallel RLC load are given in Table III. In Fig. 5, the instantaneous currents delivered by the DGu$_M$ and the three-phase load voltage are depicted from the top.

TABLE III

UNBALANCED LOAD PARAMETERS

	Phase a	Phase b	Phase c
R (Ω)	5 R	4 R	2 R
L (mH)	-	-	L

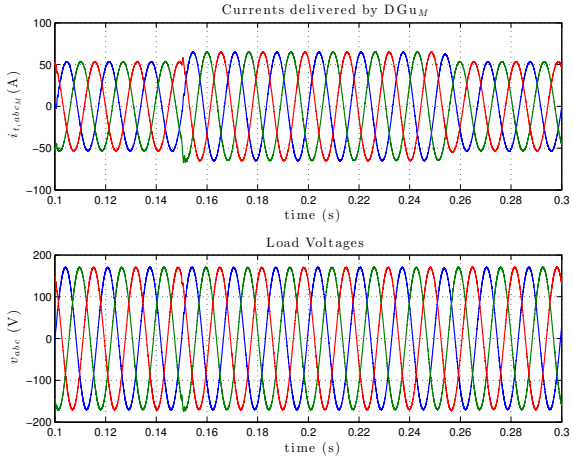

Fig. 4. Instantaneous currents delivered by the DGu$_M$ and three-phase load voltage under unknown load dynamic (balanced conditions).

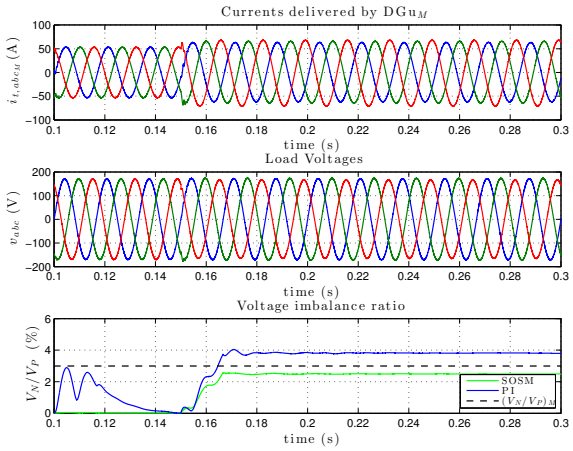

Fig. 5. From the top: instantaneous currents delivered by the DGu$_M$; load voltages under unbalanced load conditions; performance evaluation of PI and SOSM control with respect to the voltage imbalance ratio.

Moreover, to evaluate the voltage imbalance at the PCC, the percentage ratio V_N/V_P, where V_N and V_P are the magnitudes of negative and positive sequence components of PCC voltage, is calculated with the approximate formula proposed in [28]. Note that the voltage imbalance ratio obtained by using the SOSM control is almost equal to 2.5%, which is less than the maximum permissible value (3%) recommended by IEEE [29]. The imbalance ratio with PI control results almost equal to 3.9%, which is greater than the maximum permissible value. However, the proposed SOSM control strategy cannot necessarily cope with more unbalanced load conditions, but it always results significantly better than the PI control.

D. Performance under Nonlinear Load Conditions

During IOM, from $t = 0.1$ s to $t = 0.2$ s a three-phase six-pulse diode-bridge rectifier is connected to the PCC. The rectifier feeds a purely resistive load with $R = 80\,\Omega$. In Fig. 6 the instantaneous currents supplying the nonlinear load and the three-phase voltage at PCC are reported, confirming the robust stability of the proposed controller in spite of the nonlinearities introduced by the rectifier. Moreover, the Total Harmonic Distortion (THD) of load voltage is calculated. Note that the voltage THD obtained by using the SOSM control is almost equal to 1% in both transient and steady state conditions, which is less than the maximum permissible value (5%) defined by IEEE [29]. The THD with PI control in the steady state condition is almost equal to that of SOSM, while during transient the voltage THD reaches values which are greater than the maximum permissible. However, the proposed SOSM control strategy cannot necessarily cope with highly nonlinear load conditions, but it always results significantly better than the PI control during transients. Finally, in Table IV the root mean square errors of the controlled variable V_d and V_q are reported. The error is evaluated by using SOSM and PI control in IOM. The first one results in being more robust and performant than the traditional PI control.

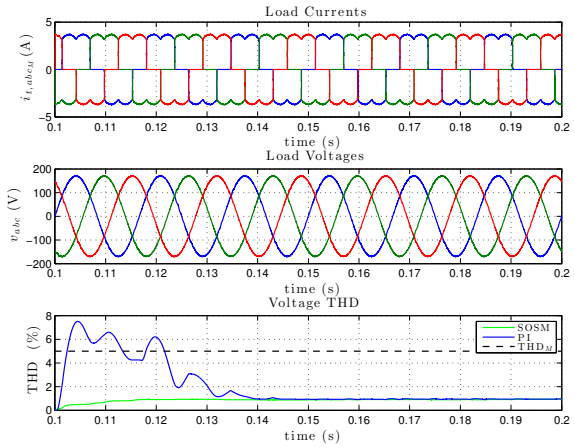

Fig. 6. From the top: instantaneous load currents; load voltages under nonlinear load conditions; performance evaluation of PI and SOSM control with respect to the voltage THD.

TABLE IV
RMS VALUES OF VOLTAGES ERROR

Case	PI	SOSM
Balanced	100%	18.5%
Unbalanced	100%	18.8%
Nonlinear	100%	20.9%

VII. CONCLUSIONS

In this paper a second order sliding mode control, belonging to the class of the so-called Suboptimal algorithms, has been proposed to regulate the voltage and current signals of a microgrid. A master-slave scheme has been designed and the control algorithms have been suitably tuned to guarantee good performance in case of islanded configuration and grid-connected mode. The stability analysis has been discussed, and satisfactory performances have been obtained in simulation relying on a three degree-of-freedoms microgrid. The proposed SOSM control strategies ensure closed-loop performance complying with the IEEE recommendations for power systems and resulting in being more robust than traditional PI control.

REFERENCES

[1] H. B. Puttgen, P. MacGregor, and F. Lambert, "Distributed generation: Semantic hype or the dawn of a new era?" *Power and Energy Magazine, IEEE*, vol. 1, no. 1, pp. 22–29, Jan 2003.

[2] R. Lasseter and P. Paigi, "Microgrid: a conceptual solution," in *Proc. 35th IEEE Power Electron. Specialists Conf.*, vol. 6, June 2004, pp. 4285–4290 Vol.6.

[3] J. Guerrero, P. C. Loh, T.-L. Lee, and M. Chandorkar, "Advanced control architectures for intelligent microgrids - part ii: Power quality, energy storage, and ac/dc microgrids," *IEEE Trans. Ind. Electron.*, vol. 60, no. 4, pp. 1263–1270, Apr. 2013.

[4] F. Katiraei, M. Iravani, and P. Lehn, "Micro-grid autonomous operation during and subsequent to islanding process," *IEEE Trans. Power Del.*, vol. 20, no. 1, pp. 248–257, Jan. 2005.

[5] R. Lasseter, "Microgrids," in *Power Engineering Society Winter Meeting, 2002. IEEE*, vol. 1, 2002, pp. 305–308 vol.1.

[6] E. Planas, A. G. de Muro, J. Andreu, I. Kortabarria, and I. M. de Alegría, "General aspects, hierarchical controls and droop methods in microgrids: A review," *Renewable and Sustainable Energy Reviews*, vol. 17, no. 0, pp. 147 – 159, 2013.

[7] O. Palizban, K. Kauhaniemi, and J. M. Guerrero, "Microgrids in active network management—part i: Hierarchical control, energy storage, virtual power plants, and market participation," *Renewable and Sustainable Energy Reviews*, vol. 36, no. 0, pp. 428 – 439, 2014.

[8] S. Amin and B. Wollenberg, "Toward a smart grid: power delivery for the 21st century," *IEEE Power Energy Mag.*, vol. 3, no. 5, pp. 34–41, Sep. 2005.

[9] P. Piagi and R. Lasseter, "Autonomous control of microgrids," in *Power Eng. Society General Meeting*, 2006, p. 8.

[10] H. Karimi, E. Davison, and R. Iravani, "Multivariable servomechanism controller for autonomous operation of a distributed generation unit: Design and performance evaluation," *IEEE Trans. Power Syst.*, vol. 25, no. 2, pp. 853–865, May 2010.

[11] M. Babazadeh and H. Karimi, "A robust two-degree-of-freedom control strategy for an islanded microgrid," *IEEE Trans. Power Del.*, vol. 28, no. 3, pp. 1339–1347, Jul. 2013.

[12] S. Riverso, F. Sarzo, and G. Ferrari-Trecate, "Plug-and-play voltage and frequency control of islanded microgrids with meshed topology," *CoRR*, vol. abs/1405.2421, 2014.

[13] G. Bartolini, A. Ferrara, and E. Usai, "Chattering avoidance by second-order sliding mode control," *IEEE Trans. Automat. Control*, vol. 43, no. 2, pp. 241–246, Feb. 1998.

[14] ——, "Output tracking control of uncertain nonlinear second-order systems," *Automatica*, vol. 33, no. 12, pp. 2203 – 2212, Dec. 1997.

[15] G. Bartolini, A. Ferrara, E. Usai, and V. Utkin, "On multi-input chattering-free second-order sliding mode control," *IEEE Trans. Automat. Control*, vol. 45, no. 9, pp. 1711–1717, Sep. 2000.

[16] G. Bartolini, A. Ferrara, and E. Usai, "On boundary layer dimension reduction in sliding mode control of siso uncertain nonlinear systems," in *Proc. IEEE Int. Conf. Control Applications*, vol. 1, Trieste, Italy, Sep. 1998, pp. 242 –247 vol.1.

[17] M. Rubagotti and A. Ferrara, "Second order sliding mode control of a perturbed double integrator with state constraints," in *Proc. American Control Conf.*, Baltimora, MD, USA, Jun. 2010, pp. 985–990.

[18] R. H. Park, "Two-reaction theory of synchronous machines - generalized method of analysis - part i," *Trans. American Instit. Electr. Eng.*, vol. 48, no. 3, pp. 716 – 727, 1929.

[19] I. Balaguer, Q. Lei, S. Yang, U. Supatti, and F. Z. Peng, "Control for grid-connected and intentional islanding operations of distributed power generation," *IEEE Trans. Ind. Electron.*, vol. 58, no. 1, pp. 147–157, Jan. 2011.

[20] G. Bartolini, A. Ferrara, A. Levant, and E. Usai, *On second order sliding mode controllers*, ser. Lecture Notes in Control and Information. London, UK: Springer-Verlag, 1999, pp. 329–350.

[21] M. Babazadeh and H. Karimi, "Robust decentralized control for islanded operation of a microgrid," in *Power and Energy Society General Meeting, 2011 IEEE*, July 2011, pp. 1–8.

[22] L. Fridman, "Singularly perturbed analysis of chattering in relay control systems," *IEEE Trans. Automat. Control*, vol. 47, no. 12, pp. 2079 – 2084, Dec. 2002.

[23] I. Boiko, L. Fridman, A. Pisano, and E. Usai, "Analysis of chattering in systems with second-order sliding modes," *IEEE Trans. Automat. Control*, vol. 52, no. 11, pp. 2085 –2102, Nov. 2007.

[24] A. Levant, "Chattering analysis," *IEEE Trans. Automat. Control*, vol. 55, no. 6, pp. 1380 –1389, Jun. 2010.

[25] I. Boiko, "Analysis of chattering in sliding mode control systems with continuous boundary layer approximation of discontinuous control," in *Proc. American Control Conf.*, San Francisco, CA, USA, Jul. 2011, pp. 757 –762.

[26] H. Lee and V. I. Utkin, "Chattering suppression methods in sliding mode control systems," *Annual Reviews in Control*, vol. 31, no. 2, pp. 179 – 188, Oct. 2007.

[27] V. I. Utkin, *Sliding Modes in Optimization and Control Problems*. New York: Springer Verlag, 1992.

[28] P. Pillay and M. Manyage, "Definitions of voltage unbalance," *IEEE Power Engineering Review*, vol. 21, no. 5, pp. 50–51, 2001.

[29] IEEE, "Recommended practice for monitoring electric power quality," *IEEE Std 1159-2009 (Revision of IEEE Std 1159-1995)*, pp. c1–81, Jun. 2009.